1 **New Insights on the Evolutionary Relationships Between the Major Lineages of**
2 **Amoebozoa**
3
4 Yonas I. Tekle[1][*], Fang Wang[1], Fiona C. Wood[1], O. Roger Anderson[2], Alexey Smirnov[3]
5
6 [1] Dept. of Biology, Spelman College, Atlanta, Georgia, USA
7 [2] Dept. of Biology and Paleo Environment, Lamont⬜Doherty Earth Observatory of
8 Columbia University, Palisades, New York, USA
9 [3] Dept. of Invertebrate Zoology, Faculty of Biology, St. Petersburg State University,
10 Russia
11
12 *Corresponding Author: Yonas I. Tekle, Spelman College, 350 Spelman Lane Southwest,
13 Atlanta, GA 30314---Telephone number: 404-270-5779; e-mail: ytekle@spelman.edu

Abstract

The supergroup Amoebozoa unites a wide diversity of amoeboid organisms and encompasses enigmatic lineages recalcitrant to modern phylogenetics. Deep divergences, taxonomic placement of some key taxa and character evolution in the group largely remain poorly elucidated or controversial. We surveyed available Amoebozoa genomes and transcriptomes to mine conserved putative single copy genes, which were used to enrich gene sampling and generate the largest supermatrix (824 genes) in the group to date. We recovered a well-resolved and supported tree of Amoebozoa, revealing novel deep level relationships and resolving placement of enigmatic lineages congruent with morphological data. In our analysis the deepest branching group is Tubulinea. A recent proposed major clade Tevosa, uniting Evosea and Tubulinea, is not supported. Based on the new phylogenetic tree, paleoecological and paleontological data as well as data on the biology of presently living amoebozoans, we hypothesize that the evolution of Amoebozoa probably was driven with the need to disrupt and graze on microbial mats - a dominant ecosystem of the mid-Proterozoic period of the Earth history.

Keywords: Amoebozoa, phylogenomics, flagellum, eukaryotes, genome, transcriptome

1 Introduction
2
3   The supergroup Amoebozoa [1] comprises a variety of amoeboid lineages; namely,
4 naked lobose amoebae (which are "archetypal" amoebae), testate lobose amoebae,
5 mycetozoans, anaerobic archamoebians and a heterogeneous assemblage of flattened
6 amoeboid, branching reticulate or flagellated organisms; presently known as Variosea.
7 Amoebozoa holds a key evolutionary position, being the closest known relative of
8 Obazoa that, among other organisms, includes humans [2,3]. Resolving the phylogenetic
9 tree of this lineage is critical for answering important questions pertaining to the
10 evolutionary origin of Amoebozoa, as well as for further clarification of the root of the
11 eukaryotic tree [3-8].
12
13   Our understanding of the evolution and taxonomy of amoeboid protist originally
14 conceived from cytological, morphological and life cycle evidence [9,10]. Early studies
15 based on small subunit rDNA (18S) gene indicated the polyphyly of naked amoebae
16 (gymnamoebae) and formed the basis of our understanding of the supergroup
17 Amoebozoa [1,11,12]. The assemblage of Amoebozoa grew in membership, albeit with little
18 improved resolution; or sometimes with conflicting hypotheses pertaining to within-
19 group relationships (e.g., [13-19]). This led to subsequent revisions and reevaluation in
20 attempts to combine morphological and molecular characters and find synapomorphic
21 characters of major clades [20-23]. While this achieved major progress in our overall
22 understanding of the group, much of the deep and intermediate relationships and
23 placement of some groups of uncertain phylogenetic affinities (so-called *incertae sedis*
24 taxa) remained elusive. Multigene studies, varying in breadth and depth of gene and
25 taxon sampling, managed to overcome many of the challenges of single-gene
26 reconstructions; and they resolved some of the long-standing evolutionary questions in
27 the group [4,24-27]. A recent phylogenomic study by Kang et al. [4] reported a deep level
28 phylogeny of Amoebozoa based on large taxon sampling. However, the placements of
29 some *incertae sedis* lineages were not entirely resolved. For some groups, other
30 phylogenomic studies reported conflicting relationships [25,26,28].
31
32   The conflict in existing phylogenomic studies can be attributed partially to
33 limitations of taxon and gene sampling as well as the methodology. Kang et al. [4] used
34 large taxon sampling, but included only a small fraction of data (325 genes), from the
35 vast amount of transcriptomic and genomic data available, based on commonly used
36 genetic markers in eukaryotes. There are data suggesting that taxon sampling alone is not
37 sufficient to resolve deep divergences in ancient lineages that might have undergone
38 rapid radiations [29]. The age of Amoebozoa is estimated to be over a billion years, and the
39 probable origin of the group is dated back to the mid-Proterozoic period [30,31]. Therefore,
40 in order to infer deep evolutionary divergences not only increased taxon sampling, but
41 also more representative genetic sampling along with the application of appropriate
42 models and methods are essential.
43
44   In this study, we sampled putative single copy gene markers from genome-wide
45 assays, increased taxon sampling and produced the largest amoebozoan supermatrix to
46 date. This large dataset enabled us to recover a well-resolved and supported tree of the

1   Amoebozoa. In addition, we uncover a well-corroborated novel deep-level relationship
2   and resolved the placement of some *incertae sedis* lineages.
3
4
5   **Results**
6
7   **The Tree of Amoebozoa**
8
9   We recovered a monophyletic tree of Amoebozoa that is well resolved and
10   supported in every one of our analyses (Figs. 1, S1-S4). Our datasets, with and without
11   fast-evolving sites removed (analyzed using the complex model in IQ-TREE) recovered
12   all well-established major subclades of Amoebozoa including Discosea, Archamoebae,
13   Cutosea, Eumycetozoa, Variosea and Tubulinea with full support (Figs. 1, S1). The two
14   well-known long-branch lineages, Archamoebae and Cutosea, were placed in their
15   respective correct phylogenetic positions without removal of fast evolving sites in our full
16   dataset (Fig. 1). Removal of fast evolving, rate categories, in IQ-TREE neither affected
17   the topology nor improved support values (Fig. S1). In the RAxML analysis, the accurate
18   placement of Archamoebae and Cutosea, required removal of six fast evolving rate
19   categories (38%) from the full dataset (Fig. S2); but resulted in the same final tree
20   configuration. The RAxML tree had generally lower supported branches but was
21   congruent with the topology of the trees inferred using IQ-TREE (Figs. 1, S1, S2). A
22   similar reduced dataset was analyzed using Bayesian inference, which yielded similar
23   topology despite lack of convergence in our PhyloBayes analysis (data not shown). Kang
24   et al. [4] also reported similar topologies among their ML and PhyloBayes trees despite
25   limited number of chains used and lack of convergence in some of their PhyloBayes
26   analyses. Due to the high computational demand, Bayesian inference was not feasible
27   with our large dataset. The consistency of tree topologies across methods and algorithms
28   used, as well as the placement of long-branch taxa (Archamoebae and Cutosea) without
29   removal of fast evolving sites in IQ-TREE (likely due to complex model used),
30   demonstrates the robustness of our result.
31
32   In our phylogenomic tree, all major clades are congruent with previous published
33   topologies [4,24-26]. Moreover, our phylogenomic tree has well-corroborated relationships;
34   and the recovery and placement of enigmatic taxa are more stable (Figs. 1, S1, S2). Our
35   results yielded improved support for the Flabellinia and Thecamoebida clades compared
36   to a previous comparable phylogenomic study [4]. We have recovered for the first time a
37   fully supported monophyletic clade encompassing two *incertae sedis* taxa, *Vermistella*
38   and *Stygamoeba*. Both these lineages were placed in the order Stygamoebida based on
39   morphological evidence [22]. The monophyly and placement of this order in the tree of
40   Amoebozoa has not been resolved in previous multigene analyses (e.g., [4]). In our tree
41   Stygamoebida clade forms a sister group relationship with Thecamoebida with full
42   support (Fig. 1). We also find some discrepancies between our tree (Fig. 1) and that of
43   Lahr et al. [5] in the branching order of the Tubulinea clade, albeit with similar taxon
44   sampling for this clade. Our analysis shows clade Corycida as the most basal Tubulinea
45   lineage similar to that of Kang et al. [4] phylogeny (Fig. 1). *Nolandella* sp., a member of

1 Euamoebida, did not group with *Amoeba proteus* and *Copromyxa protea* in our analysis,
2 but formed an independent lineage (Fig. 1).
3
4
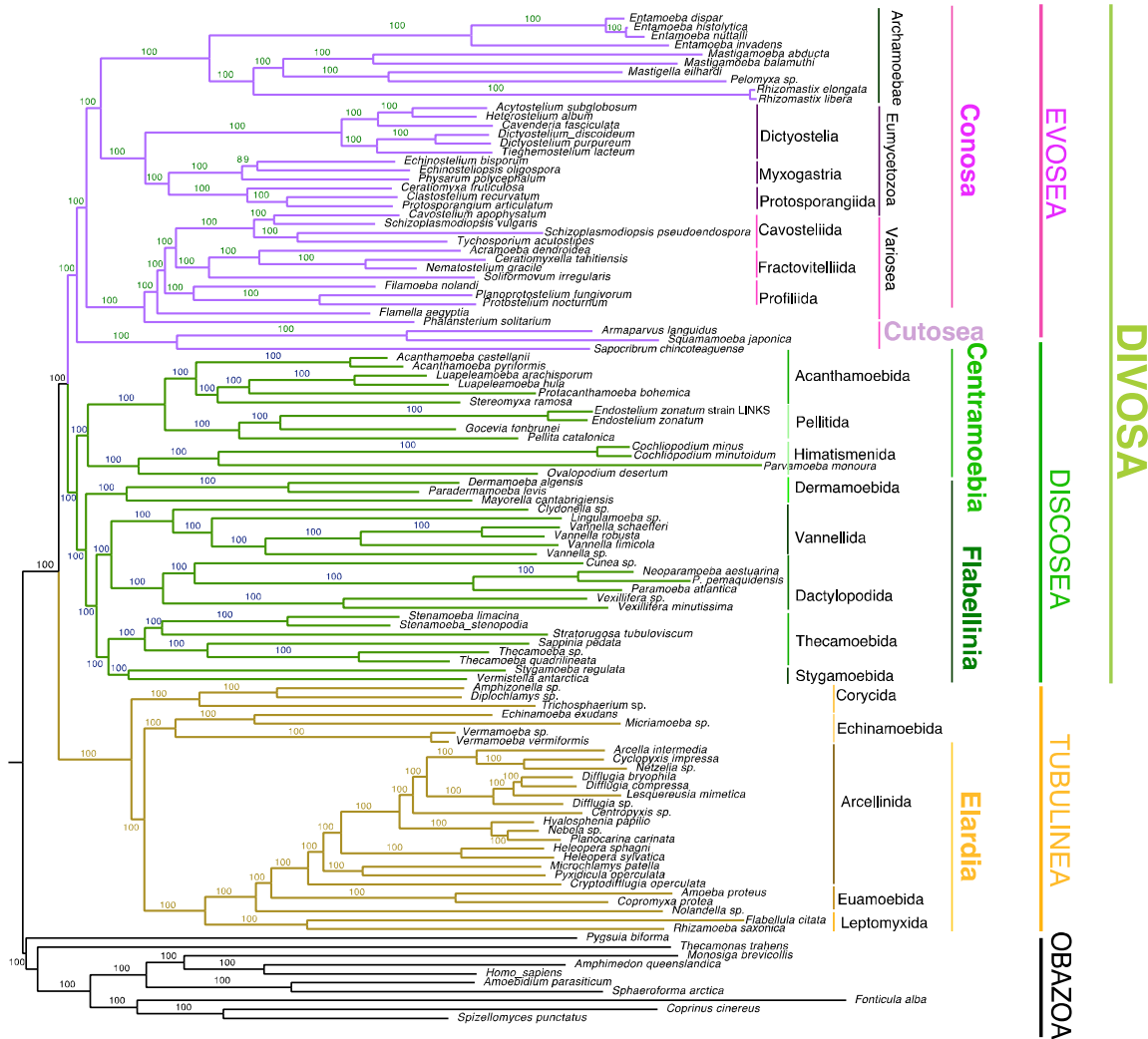
5
6 **Figure 1.** Genome wide phylogeny of the Amoebozoa inferred using Maximum
7 likelihood (ML) in IQ-TREE with LG+G4+C60+F model of evolution. The data matrix
8 used to infer this tree consisted of 113,910 amino acid sites from the full dataset, derived
9 from 824 genes and 113 taxa including 10 outgroup taxa. Clade supports at nodes are ML
10 IQ-TREE 1000 ultrafast bootstrap values obtained using the same model. All branches
11 are drawn to scale except a branch leading to Archamoebae, and *Sapocribrum*
12 *chincoteaguense* and *Parvamoeba monoura*, that were reduced to one-third and half,
13 respectively.
14

A Novel Deep Split of the Amoebozoa

16
17   Our analysis for the first time revealed a novel, well-supported deep spilt of
18 Amoebozoa; not reported in previous phylogenomic studies. Amoebozoa is split into two
19 fully supported major subclades: Tubulinea and a second one comprised of the remaining

5

1   major subclades including Evosea (Eumycetozoa, Variosea, Archamoebae, and Cutosea)
2   and Discosea (Figs. 1, S1, S2). This branching is different from a finding in a recent
3   phylogenomic study that reported a spilt between Discosea and Tevosa
4   (Evosea+Tubulinea) [4]. Tevosa is not supported in our analyses, including analyses with
5   removal of fast sites. On the other hand, the deep split (Evosea+Discosea *vs.* Tubulinea)
6   observed in our phylogenomic tree is supported in all analyses of our data sets. The deep
7   spilt receives almost full support in our internode certainty (IC) analyses as implemented
8   in QuartetScores (1.00) and RAxML (0.979) (Figs. S3, S4). AU test of our topology,
9   comparing alternative topologies with Tevosa and a traditional deep relationship uniting
10   Discosea and Tubulinea (Lobosa), showed that the newly recovered deep spilt has the
11   highest p-value (p-AU = 0.947). Hypothesis Lobosa was rejected (p-AU = 0.000278),
12   while Tevosa cannot be rejected with p-value just above threshold (p-AU = 0.0564). For
13   convenience, we suggest a new name for the deep spilt (Discosea+Evosea) clade; i.e.,
14   Divosa, a term derived from a combination of the name of the two clades.
15
16
17   **Discussion**
18
19   **Targeted Genome-Wide Data Enrichment for Phylogenomics of Amoebozoa**
20
21   Despite the large number of RNA-Seq data generated in recent studies [4,24-26], only
22   a small fraction of this data has been utilized in phylogenomic analyses. To increase it,
23   we compiled a total of 1559 markers using genome-derived protein coding genes from
24   113 amoebozoan genomes and transcriptomes. Using putative single copy markers,
25   primarily derived from Amoebozoa genomes, has enabled us to introduce highly
26   conserved markers with phylogenetic signal corroborating morphology- and
27   phylogenomic-based amoebozoan hypotheses [4,24]. While single-copy genes identified in
28   some genomes might not always apply to others, a previous phylogenomic study with
29   seed plants, based on single copy markers resulted in more resolved phylogeny both at
30   shallow and deep nodes [32]. In this study, we followed a stringent approach aided by
31   automated and manual curation of markers, selected from the above-mentioned dataset to
32   build the largest supermatrix (823 genes) in the Amoebozoa. With this approach, we
33   substantially increased the total number of genes used in Amoebozoa phylogenomics.
34   Our analysis yielded consistent and well-corroborated topologies, despite whether we
35   included or excluded fast evolving sites (Figs. 1, S2). The robustness of our phylogeny is
36   also corroborated with the high support values from internode certainty analysis (Figs.
37   S3, S4). One of the evident results of this approach is the first time phylogenomic
38   recovery of the monophyly of the taxon Stygamoebida, earlier supported only at the
39   morphological level [22,23] and a recovery of a novel deep split divergence of Amoebozoa.
40
41   **Unraveling deep divergence of Amoebozoa**
42
43   A recent phylogenomic study by Kang et al. [4], though based on a slightly smaller
44   taxon sampling, proposed a split of the Amoebozoa supergroup into two major subclades:
45   Tevosa (Evosea+Tubulinea) and Discosea. By contrast, in our study Evosea robustly
46   groups as sister clade to Discosea (Figs. 1, S1, S2). Both phylogenetic hypotheses,

1 'Tevosa' and Divosa, receive high statistical support in their and our study, respectively
2 (see Fig. 1, [4]). In phylogenomic analyses, it is common to see that short subtending deep
3 nodes receive high statistical support [33]. Amoebozoan deep nodes are characterized by
4 very short branch lengths, an indication of limited supporting characters, or possible
5 ancient rapid diversification. Strong statistical support at these levels of nodes does not
6 necessarily mean that the inferred relationships are correct. Statistical indices such as
7 bootstrap values and Bayesian posterior probabilities only assess sampling effects, and
8 give an indication of tree reliability that is dependent on the data and the method [34]. This
9 can partially explain why these short-branch, deep nodes in Amoebozoa phylogenomic
10 studies tend to collapse, or vary, depending on the method of analysis or the composition
11 of the gene/taxon sampling [4,24-26]. Certainly, caution still must be taken when interpreting
12 ancient divergences, because results can be muddied by noise (e.g., gene history [35] or lack
13 of signal due to rapid radiation [29]). However, the support of the split recovered in the
14 present study is high and originates from different lines of evidence.
15
16   It is possible to note that in many lineages trophozoites of Discosea and Variosea
17 are more similar to each other rather than to Tubulinea. Certainly, the morphology of
18 presently living amoeboid organisms is derived and adaptive, but generally it is possible
19 to say that members of Divosa lineage share more morphological similarity between each
20 other rather than with the Tubulinea lineage. For example, amoebae of the genus
21 *Flamella,* belonging to the class Variosea, by their morphology may be easily confused
22 with some discosean amoebae (e.g., [36]); the same is true for individual trophozoites of
23 many mycetozoan species, showing flattened body shape and pointed subpseudopodia
24 [37,38]. Cells of amoebae belonging to the genus *Squamamoeba* (the taxon of Cutosea),
25 sometimes resemble *Korotnevella* (Discosea) in their overall morphology, hence, being
26 differently organized at the cytological level [39]. At the same time, none of discosean or
27 variosean lineages show the morphology resembling that of, e.g. Amoebida, or alteration
28 of the locomotive morphology from flattened to tubular, which is a general characteristic
29 of Tubulinea [20,22]. To certain extent, the return to the tubular body shape, subcylindrical
30 in cross-section occurs among amoeboid representatives of Archamoebea; however, this
31 might be mostly related with their specific lifestyle (parasites or pelobionts). In addition
32 the pattern of pseudopod formation (e.g., the tendency to show eruption of the hyaline
33 cytoplasm in the frontal area of the cell) makes them to be significantly different from
34 that in Tubulinea (see [40]).

35 **Mid-Proterozoic environment – the driving force for the origin of Amoebozoa**

36   The flagellum (cilium) is a highly conserved complex structure that is believed to
37 have originated only once, and be ancestral to all eukaryotes [2,41,42]. Amoebozoa are
38 remarkable in that the two basal phylogenetic lineages, Tubulinea and Discosea, have
39 entirely lost cilia, kinetosomes (basal bodies) and associated root structures; while a
40 derived major clade, Evosea, contains a handful of ciliated lineages in a few branches
41 intermingled among amoeboid lineages [21,22]. The loss of cilia and associated structures in
42 the majority members of Amoebozoa is one of the biggest mysteries pertaining to their
43 origin and evolution.

1   In ciliated members of Amoebozoa, the ciliary apparatus is characterized by a
2 specific arrangement of root structures, which includes an incomplete (Variosea and
3 Mycetozoa) or complete (Archamoebea) cone of microtubules extending from the
4 kinetosome to the nucleus [43]. In early interpretations, this conical arrangement of
5 microtubules was considered to be homologous to the ciliary root system of
6 Opisthokonta; which, together with other morphological and molecular evidence, gave
7 rise to the "Unikonta" hypothesis [2,44,45]. In this model, the hypothetical ancestor of
8 Amoebozoa was considered to be an organism with a single emergent cilium, resembling
9 *Phalansterium* or *Mastigamoeba* in cellular organization [46,47]. This lineage, combining
10 Amoebozoa and Opisthokonta, has been proposed as an alternative to that of the bikonts,
11 with two emerging cilia; which included the rest of the eukaryotic groups. Cavalier-Smith
12 [2] argued that among unikonts, paired kinetosomes (when present) resulted from
13 convergent evolution rather than common ancestry with bikonts. Molecular and
14 morphological analyses provided certain indications that the microtubular structures in
15 Amoebozoa, and Opisthokonta may not be homologues [43,48]. However, further
16 development of molecular phylogeny provided evidence for the basal position of bikont
17 organisms in the tree of eukaryotes [3,49,50]. Thereafter, the general consensus nowadays is
18 that hypothetical common ancestor of Amoebozoa, was a bikont organism [43,51,52].
19 Several authors (e.g., [3,43,49,50]) hypothesised that the presumable common ancestor was a
20 ventrally grooved biciliate gliding flagellate, capable of producing filose ventral
21 pseudopodia and possessing a relatively complex organization of the cell. That is, a cell
22 possessing two cilia with kinetosomes and root structures, ventral groove supported with
23 microtubules and dorsal pellicle – the so called "sulcozoan ancestor". Its name originates
24 from Sulcozoa – a phylum of protists established by Cavalier-Smith [43] that combines a
25 heterogenous assemblage of early evolving eukaryotic lineages. Cavalier-Smith
26 suggested that "opisthokonts and Amoebozoa evolved from sulcozoan ancestors by two
27 independent losses of the pellicular dense layers and of the ventral groove, which in both
28 cases would allow pseudopods to develop anywhere on the cell surface" (op. cit.).

29   The origin and further evolution of Amoebozoa in this hypothesis presumes the
30 loss of both cilia and kinetosomes in Lobosa (Tubulinea and Discosea) and of the
31 posterior cilium and one kinetosome in most of the ancestors of Conosa - Archamoebae,
32 Variosea and Eumycetozoa; Cutosea were not known at that time (e.g., [3,49,50]). This
33 evolutionary scenario was rather logical and is illustrated in Figure 2A. However, the
34 Lobosa/Conosa dichotomy was doubted based on some 18S gene phylogenies [27]; and it
35 subsequently failed to garner support in wide-scale phylogenomic studies [4,24,25], as well
36 as in the present study. This makes the model of multiple losses more complicated,
37 because under the new tree configuration, we have to suggest subsequent partial or
38 complete loss of cilia and related structures in all but one branch of Amoebozoa. This
39 hypothetical scenario is illustrated in Figure 2B. It remains unclear why the hypothesized
40 ancestor of Amoebozoa, being initially a quite complex biciliated organism, underwent
41 such a massive loss (or substantial simplification) of cilia-related structures in almost all
42 evolutionary lineages of Amoebozoa, and what was the driving force for such a
43 reduction.

44
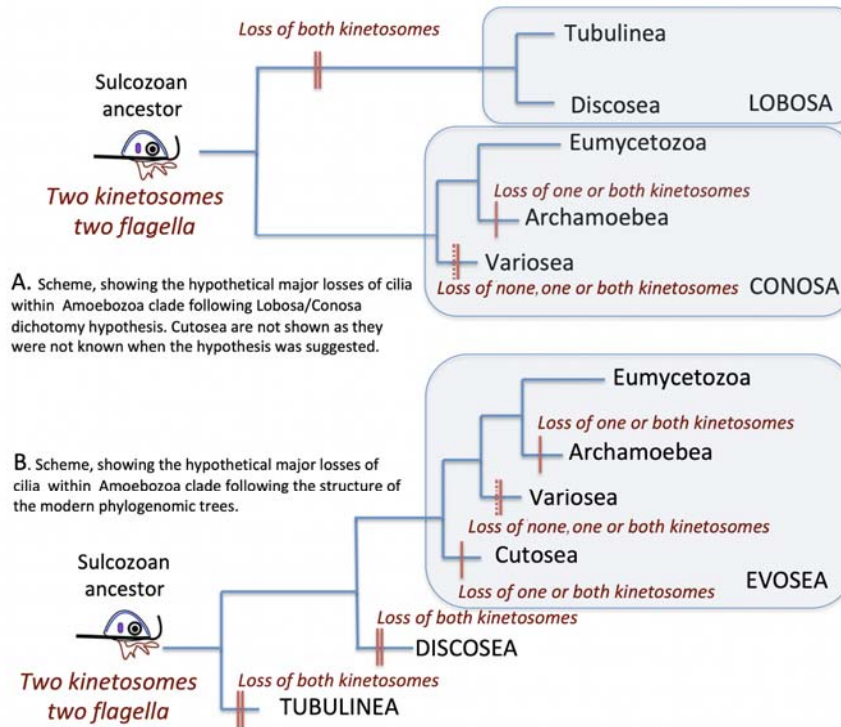
Figure 2. A scheme illustrating the loss of kinetosomes and cilia under the different evolutionary hypotheses (A and B). Vertical hash marks on branches show loss of kinetosomes (the number lost as designated by labels on the diagram) depending on the lineage.

Several studies based on molecular dating analysis correspondingly placed the origin of Amoebozoa to the Mesoproterozoic period, which means 1250 – 1624 mya [31,53]. It means that the early evolution of Amoebozoa took place at the period when the biosphere was dominated with microbial biofilms – sheets of bacteria, embedded in extracellular polymeric substances, covering almost every possible substrate [54]. Being initially rather simple, biofilms further evolved in complex microbial mats, comprising different prokaryotic organisms, showing concerted activities and intimate interactions between various microbial metabolisms [55]. The oldest mats are dated to approximately 3.5 billion years ago, and the noonday of mats covers the mid-Proterozoic period [56,57], which roughly corresponds to the estimate of the potential age of Amoebozoa.

Formation of a microbial biofilm, among other structural and biogeochemical features, can be explained as an adaptation that increases survival of bacteria to avoid predation [58,59]. The probable size of the bacterivorous biflagellate ancestor of Amoebozoa was relatively small, likely no larger than that of the existing representatives of the CRuMs clade (e.g., *Mantamonas*) or 'Excavates' (metamonads or *Malawimonas*), which is within the general size range of 2-20 µm. These organisms were able to phagocytize solitary bacteria, but consumption of microorganisms embedded in an intact microbial mat probably was beyond their capacity, as well as this is beyond the capacity of the modern flagellates of comparable size [60,61]. Feeding on bacteria, major constituents of the

9

1 microbial mats (the dominant food source in the mid-Proterozoic environment), required
2 increment in the body size and acquisition of special adaptations allowing them to ingest
3 filamentous food. However, the latter was again related to the body size, because the
4 filament, even compacted in some way, must be ingested – i.e., appear inside the cell.

5   Due to Reynolds number limitation [62,63], the increment in the body size makes
6 ciliary motility less adaptive due to loss of efficiency. Thus, from an adaptive aspect, an
7 amoeboid lifestyle might be a way to increase the body size while retaining a motility
8 function, no longer dependent on cilia. An amoeboid organization also could gain the
9 adaptive capacity to disrupt microbial mats and graze, feeding on bacteria within the
10 mats. This adaptation would provide access to the dominant food source in the biosphere
11 of the mid-proterozoic eon. Indeed, presently, naked amoebae are known as one of the
12 primary grazers of bacterial biofilms [64-66]. Moreover, they not only just graze and
13 phagocytize prey in the mats, but also disrupt them, making their content available for
14 other organisms [67,68]. Finally, in addition to the advantage of feeding on bacterial mats
15 [69,70], it is also possible that an increase in body size alleviated pressure of predation by
16 other organisms on the last Amoebozoan common ancestor (LACA), which for some
17 time provided it an adaptive advantage and allowed rapid proliferation and differentiation
18 of Amoebozoa in the mid-Proterozoic environment.

19   Hence, we hypothesise that the adaptive value of amoeboid locomotion and
20 concomitant grazing potential on the dominant food source in the mid-proterozoic
21 biosphere – the microbial mats – favoured the evolution of the Amoebozoa. They
22 probably successfully solved this task by the increment of body size. However, at the
23 same time, the efficiency of flagellar locomotion was highly reduced or lost; and this
24 resulted in the multiple suspensions of the flagellar apparatus, which is completely absent
25 in two major current amoebozoan lineages – Tubulinea and Discosea (Fig. 2). The
26 modern configuration of the Amoebozoan tree, which rejects the Lobosa/Conosa
27 dichotomy and suggests a subsequent branching of lineages (with either Tubulinea or
28 Discosea at the base), leaves open a major question. That is, was the last Amoebozoa
29 common ancestor an amoeboflagellate, with the domination of amoeboid movement
30 based on the microtubular cytoskeleton; or was the flagellum-related structures and
31 microtubular locomotive system entirely suppressed? If the latter case is true, then it
32 probably drove the ancestral amoebozoan to switch to the acto-myosin movement, as
33 found in modern representatives of naked and testate lobose amoebae. Probably, the
34 answer to this question may be obtained by the analysis of gene content and the level of
35 flagellum-related gene expression in the amoebozoan genomes. However, the dataset
36 available for quality analysis remains limited in this group of protists and requires further
37 accumulation prior to conclusive study.
38
39 **Methods**
40
41 **Transcriptome Assembly and Contamination Examination**
42
43   All transcriptome data used in this study were assembled using a bioinformatics
44 pipeline described in Tekle and Wood [25]. As a precautionary measure for contamination,

1 high-quality data generated from single cell or monoclonal cultures, and without history
2 of contamination, were prioritized in our data collection. We also checked highly
3 conserved genes (e.g., small subunit rDNA and cytoskeletal genes) for assembled
4 transcriptomes to check the identity of the species. Species suspected to have been
5 contaminated (e.g., *Ripella* sp. DP13-Kostka) or with low- or poor-quality transcriptome
6 data (see below) have been removed from the final analysis. Assembled contigs were
7 translated into protein sequences using TransDecoder
8 (https://github.com/TransDecoder/TransDecoder/wiki).
9
10 **Taxon and gene sampling**
11
12   A total of 107 amoebozoans representing the vast diversity of the supergroup and
13 10 outgroup taxa from a closely related clade, Obazoa, were included in our initial
14 analysis (Table S1). Four ingroup taxa including *Parvamoeba rugata*, *Centropyxis*
15 *aculeata*, *Hyalosphenia elegans* and *Grellamoeba robusta,* were removed from the final
16 dataset due to poor data quality. A recent phylogenomic study [5] that focused on testate
17 amoebae (clade Tubulinea) reported a topology of Tubulinea that differed from that of
18 Kang et al. [4]. To explore these discrepancies further, and assess the impact of taxon
19 sampling on branching order of Tubulinea clade and its position within the Amoebozoa
20 phylogeny, we added more slowly evolving taxa to Tubulinea. The final supermatrix
21 consisted of 113 taxa including the outgroup taxa (Table S1).
22
23   A genome wide gene sampling approach using available amoebozoan genomes
24 was employed to identify single copy markers. Previous phylogenomic studies have used
25 conserved phylogenetic markers commonly found in a wide range of eukaryotic diversity
26 [4,24]. In this study we used a series of bioinformatics steps to maximize gene sampling in
27 the Amoebozoa. We conducted a whole genome comparison of three well-annotated
28 amoebozoan genomes, *Acanthamoeba castellanii*, *Dictyostelium discoideum* and
29 *Entamoeba histolytica,* to extract commonly shared protein-coding genes among these
30 genomes in OrthoVenn [71]. Inclusion of *E. histolytica* greatly reduced the number of
31 shared genes by 40% because this amitochondriate parasitic species has a comparably
32 much reduced genome to the free-living amoebae. For this reason, to be more
33 representative, further comparative analysis was done using *A. castellanii* and *D.*
34 *discoideum* as reference genomes to mine single-copy genes. Using this approach, we
35 identified 1559 putative single copy genes that were used as a query to search
36 orthologous genes from ingroup and outgroup taxa.
37
38   We used NCBI-BLAST with e-value threshold of 10^{-15} to retrieve homologous
39 sequences from transcriptomes or genomes of our selected taxa. From this analysis,
40 sequences with best e-value scores were retained for each taxon. The retained sequences,
41 for each taxon and gene, were compiled and aligned using a sequence alignment tool,
42 MAFFT, with default setting [72]. These alignments were then trimmed in TrimAl [73] using
43 "automated1" setting provided by the program. To inspect potential paralogs from each
44 gene, we inferred single gene trees using IQ-TREE with the best-fit model automatically
45 fast selected by ModelFinder [74]. Both single gene trees and their corresponding
46 alignments were then inspected manually for paralogy and other anomalies related to

1   alignment accuracy, sequence length and fast evolving lineages ((Single gene alignment
2   and trees available for review on this link: https://www.dropbox.com/). We applied strict
3   gene selection criteria that included removal of anomalous grouping (e.g., lineages that
4   grouped with outgroup or wrong (unexpected) phylogenetic position with >90%
5   bootstrap support) and genes that showed paralogy (duplication) signs. To mitigate the
6   impact of long-branch attraction during phylogenetic reconstruction, we removed genes
7   that contained three or more long-branch lineages. Two exceptions for this approach were
8   the well-known long-branch lineages, Cutosea and *Entamoeba*, that were kept in all of
9   our analyses. These two lineages were retained since all their representatives are mostly
10   long-branches. They are also indirect indicators of noise in a data matrix since their
11   correct placement usually requires removal of fast-evolving sites due to the effect of
12   long-branch attraction. Following these criteria, we retained a total of 824 gene clusters
13   in the final dataset. Orthologous group numbers were assigned for each gene cluster using
14   ublast in USEARCH [75] with e-value 10^{-10}. We used the OrthoMCL database to generated
15   ortholog group numbers [76] (Table S2).
16
17   **Supermatrix Construction and Tree Inference**
18
19   The alignments from 824 genes were concatenated into an initial supermatrix
20   containing 198,280 amino acid sites and 117 taxa using a customized R script. Taxa with
21   over 80% gappy sites were removed, which resulted in exclusion of 4 lineages
22   (*Parvamoeba rugata*, *Centropyxis aculeata*, *Hyalosphenia elegans*, *Grellamoeba*
23   *robusta*). Constant sites, and sites with more than 50% missing data, were removed from
24   this alignment, and the resulting supermatrix retained 113,910 amino acid sites and 113
25   taxa for the full dataset.
26
27   Phylogenomic analyses of the final datasets were conducted in IQ-TREE – an
28   efficient tool to analyze large datasets by the maximum likelihood (ML) method [74]. All
29   IQ-TREE analyses were preformed using LG+G4+C60+F model, with 1000 replicates
30   for ultrafast bootstrap, which allowed full profile mixture model C60 and Gamma rate
31   heterogeneity across sites. We also analyzed our dataset in RAxML v.8.2.X [77] using
32   PROTGAMMALG4X model; branch support was estimated from 1000 rapid bootstrap
33   pseudoreplicates.
34
35   Fast-evolving sites and taxa are known to be problematic for tree inference due to
36   saturation of substitutions and subsequent convergent evolution resulting in long-branch
37   attraction (LBA) and other systematic errors. To test the effects of these types of errors
38   on our phylogenomic analysis, we performed a site removal assay in which each site of
39   the supermatrix was assigned to one of 16 categories based on its rate from IQ-TREE.
40   This was performed using a posterior mean site frequency (PMSF) model with mixture
41   model C60 and 16 discrete rate categories of sites. For this analysis, we used the tree
42   from full dataset inferred above as a guide tree. The impact of fast evolving sites on
43   resulting phylogenies was assessed by subsequent removal of fast categories of sites (up
44   to 6 categories). In IQ-TREE our full dataset was analyzed with 3 categories removed
45   using PMSF model with a guide tree inferred from the complex model (LG+G4+C60+F)

12

1 mentioned above. In RAxML, 3 and 6 fast site categories were removed and analyzed
2 using the same model as above.
3
4 **Internode Certainty Analysis and Hypothesis Testing**
5
6   As alternative to bootstrap branch support from IQ-TREE, we calculated
7 internode certainty (IC) scores using the program QuartetScores [78]. This approach
8 calculated IC scores from the frequencies of quartets, which can correct for the missing
9 taxa using a set of trees. For this analysis, we used 1000 bootstrap trees generated from
10 LG+G4+C60+F model in IQ-TREE with our full dataset. Alternatively, we used RAxML
11 to estimate the degree of certainty for internodes and tree topology for bipartitions with
12 PROTGAMMALG4X model [79].
13
14   We used Approximately Unbiased (AU) tests [80] to test alternate tree topologies
15 pertaining to the deep node hypotheses Divosa (this study), Tevosa (Kang et al. 2017)
16 and Lobosa [27] with the full dataset (113,910 sites). Two loosely constrained topologies
17 Tevosa ([Tubulinea+Evosea]+Discosea) and Lobosa ([Discosea+Tubulinea]+Evosea)
18 were optimized under LG+G4+F+C60 in IQ-TREE. These optimized trees were
19 compared with our tree (Divosa, ([Discosea+Evosea], Tubulinea) using AU test with
20 10,000 RELL bootstrap replicates [81]. The hypotheses that had p-AU ≥ 0.05 within the
21 95% confidence interval could not be rejected.
22
23
24 **References**
25

26 1   Cavalier-Smith, T. A revised six-kingdom system of life. *Biological Reviews of*
27   *the Cambridge Philosophical Society* **73**, 203-266 (1998).
28 2   Cavalier-Smith, T. The phagotrophic origin of eukaryotes and phylogenetic
29   classification of protozoa. *International Journal of Systematic and Evolutionary*
30   *Microbiology* **52**, 297-354 (2002).
31 3   Brown, M. W. *et al.* Phylogenomics demonstrates that breviate flagellates are
32   related to opisthokonts and apusomonads. *Proc Biol Sci* **280**, 20131755,
33   doi:10.1098/rspb.2013.1755 (2013).
34 4   Kang, S. *et al.* Between a Pod and a Hard Test: The Deep Evolution of Amoebae.
35   *Mol Biol Evol* **34**, 2258-2270, doi:10.1093/molbev/msx162 (2017).
36 5   Lahr, D. J. G. *et al.* Phylogenomics and Morphological Reconstruction of
37   Arcellinida Testate Amoebae Highlight Diversity of Microbial Eukaryotes in the
38   Neoproterozoic. *Curr Biol* **29**, 991-1001 e1003, doi:10.1016/j.cub.2019.01.078
39   (2019).
40 6   Yoon, H. S. *et al.* Broadly sampled multigene trees of eukaryotes. *BMC*
41   *Evolutionary Biology* **8**, 14 (2008).
42 7   Burki, F. *et al.* Phylogenomics reshuffles the eukaryotic supergroups. *PLoS ONE*
43   **2**, e790 (2007).
44 8   Parfrey, L. W. *et al.* Broadly sampled multigene analyses yield a well-resolved
45   eukaryotic tree of life. *Systematic biology* **59**, 518-533, doi:syq037 [pii]
46   10.1093/sysbio/syq037 (2010).

9   Page, F. C. The classification of 'naked' amoebae (Phylum Rhizopoda). *Arch. Protistenkd.* **133**, 199–217 (1987).

10   Rogerson, A. & Patterson, D. J. The Naked Ramicristate Amoebae (Gymnamoebae). *In: Lee, J.J., Leedale, G.F., Bradbury, P. (Eds.), An Illustrated Guide to the Protozoa, 2nd ed. Society of Protozoologists, Lawrence, Kansas*, pp. 1023–1053 (2002).

11   Amaral Zettler, L. A. *et al.* Microbiology: Eukaryotic diversity in Spain's River of Fire. *Nature* **417**, 137 (2002).

12   Cavalier-Smith, T. & Chao, E. E. Molecular phylogeny of the free-living archezoan Trepomonas agilis and the nature of the first eukaryote. *Journal Of Molecular Evolution* **43**, 551-562 (1996).

13   Tekle, Y. I. *et al.* Phylogenetic placement of diverse amoebae inferred from multigene analyses and assessment of clade stability within 'Amoebozoa' upon removal of varying rate classes of SSU-rDNA. *Molecular phylogenetics and evolution* **47**, 339-352 (2008).

14   Fahrni, J. F. *et al.* Phylogeny of lobose amoebae based on actin and small-subunit ribosomal RNA genes. *Mol Biol Evol* **20**, 1881-1886, doi:10.1093/molbev/msg201 (2003).

15   Nikolaev, S. I. *et al.* The testate lobose amoebae (order Arcellinida Kent, 1880) finally find their home within Amoebozoa. *Protist* **156**, 191-202 (2005).

16   Fiore-Donno, A. M., Meyer, M., Baldauf, S. L. & Pawlowski, J. Evolution of dark-spored Myxomycetes (slime-molds): molecules versus morphology. *Mol Phylogenet Evol* **46**, 878-889, doi:10.1016/j.ympev.2007.12.011 (2008).

17   Berney, C. *et al.* Expansion of the 'Reticulosphere': Diversity of Novel Branching and Network-forming Amoebae Helps to Define Variosea (Amoebozoa). *Protist* **166**, 271-295, doi:10.1016/j.protis.2015.04.001 (2015).

18   Amaral Zettler, L. A. *et al.* A molecular reassessment of the leptomyxid amoebae. *Protist* **151**, 275-282 (2000).

19   Bolivar, I., Fahrni, J. F., Smirnov, A. & Pawlowski, J. SSU rRNA-based phylogenetic position of the genera *Amoeba* and *Chaos* (Lobosea, Gymnamoebia): The origin of gymnamoebae revisited. *Molecular Biology and Evolution* **18**, 2306-2314 (2001).

20   Smirnov, A. *et al.* Molecular phylogeny and classification of the lobose amoebae. *Protist* **156**, 129-142 (2005).

21   Cavalier-Smith, T., Chao, E. E. Y. & Oates, B. Molecular phylogeny of Amoebozoa and the evolutionary significance of the unikont *Phalansterium*. *European Journal of Protistology* **40**, 21-48 (2004).

22   Smirnov, A. V., Chao, E., Nassonova, E. S. & Cavalier-Smith, T. A revised classification of naked lobose amoebae (Amoebozoa: lobosa). *Protist* **162**, 545-570, doi:S1434-4610(11)00031-9 [pii]10.1016/j.protis.2011.04.004 (2011).

23   Adl, S. M. *et al.* Revisions to the Classification, Nomenclature, and Diversity of Eukaryotes. *J Eukaryot Microbiol* **66**, 4-119, doi:10.1111/jeu.12691 (2019).

24   Tekle, Y. I. *et al.* Phylogenomics of 'Discosea': A new molecular phylogenetic perspective on Amoebozoa with flat body forms. *Mol Phylogenet Evol* **99**, 144-154, doi:10.1016/j.ympev.2016.03.029 (2016).

25   Tekle, Y. I. & Wood, F. C. Longamoebia is not monophyletic: Phylogenomic and cytoskeleton analyses provide novel and well-resolved relationships of amoebozoan subclades. *Mol Phylogenet Evol* **114**, 249-260, doi:10.1016/j.ympev.2017.06.019 (2017).

26   Cavalier-Smith, T., Chao, E. E. & Lewis, R. 187-gene phylogeny of protozoan phylum Amoebozoa reveals a new class (Cutosea) of deep-branching, ultrastructurally unique, enveloped marine Lobosa and clarifies amoeba evolution. *Mol Phylogenet Evol* **99**, 275-296, doi:10.1016/j.ympev.2016.03.023 (2016).

27   Cavalier-Smith, T. *et al.* Multigene phylogeny resolves deep branching of Amoebozoa. *Molecular phylogenetics and evolution* **83**, 293-304, doi:10.1016/j.ympev.2014.08.011 (2015).

28   Tekle, Y. I. & Williams, J. R. Cytoskeletal architecture and its evolutionary significance in amoeboid eukaryotes and their mode of locomotion. *R Soc Open Sci* **3**, 160283, doi:10.1098/rsos.160283 (2016).

29   Shin, S. *et al.* Taxon sampling to address an ancient rapid radiation: a supermatrix phylogeny of early brachyceran flies (Diptera): Diptera evolution and supermatrix. *Systematic Entomology*, doi:DOI: 10.1111/syen.12275 (2017).

30   Eme, L., Sharpe, S. C., Brown, M. W. & Roger, A. J. On the age of eukaryotes: evaluating evidence from fossils and molecular clocks. *Cold Spring Harb Perspect Biol* **6**, doi:10.1101/cshperspect.a016139 (2014).

31   Parfrey, L. W., Lahr, D. J., Knoll, A. H. & Katz, L. A. Estimating the timing of early eukaryotic diversification with multigene molecular clocks. *Proc Natl Acad Sci U S A* **108**, 13624-13629, doi:10.1073/pnas.1110633108 (2011).

32   Li, Z. *et al.* Single-Copy Genes as Molecular Markers for Phylogenomic Studies in Seed Plants. *Genome Biol Evol* **9**, 1130-1147, doi:10.1093/gbe/evx070 (2017).

33   Smith, S. A., Moore, M. J., Brown, J. W. & Yang, Y. Analysis of phylogenomic datasets reveals conflict, concordance, and gene duplications with examples from animals and plants. *BMC Evol Biol* **15**, 150, doi:10.1186/s12862-015-0423-0 (2015).

34   Delsuc, F., Brinkmann, H. & Philippe, H. Phylogenomics and the reconstruction of the tree of life. *Nat Rev Genet* **6**, 361-375, doi:10.1038/nrg1603 (2005).

35   Maddison, W. P. Gene trees in species trees. *Systematic Biology* **46**, 523-536 (1997).

36   Michel, R. & Smirnov, A. V. The genus Flamella Schaeffer, 1926 (Lobosea, Gymnamoebia), with description of two new species. . *Eur J Protistol*, 400–410 (1999).

37   Dykova, I., Lom, J., Dvorakova, H., Peckova, H. & Fiala, I. Didymium-like myxogastrids (class Mycetozoa) as endocommensals of sea urchins (Sphaerechinus granularis). *Folia Parasitol (Praha)* **54**, 1-12 (2007).

38   Fiore-Donno, A. M., Tice, A. K. & Brown, M. W. A Non-Flagellated Member of the Myxogastria and Expansion of the Echinosteliida. *J Eukaryot Microbiol* **66**, 538-544, doi:10.1111/jeu.12694 (2019).

39   Kudryavtsev, A., Pawlowski, J. Squamamoeba japonican. g. n. sp. (Amoebozoa): a deep-sea amoeba from the Sea ofJapan with a novel cell coat structure. . *Protist* **164**, 13–23 (2013).

40   Goodkov, A. V. & Seravin, L. N. Ultrastructure of the 'giant amoeba' Pelomyxa palustris. III. The vacuolar system; its nature, organization, dynamics and functional significance. . *Tsitologiya* **33**, 17–25 (in Russian with English summary) (1991).

41   Leadbeater BCS & Green, J. *The flagellates*. (Taylor and Francis, 2000).

42   Mitchell, D. R. The evolution of eukaryotic cilia and flagella as motile and sensory organelles. *Adv Exp Med Biol* **607**, 130-140, doi:10.1007/978-0-387-74021-8_11 (2007).

43   Cavalier-Smith, T. Early evolution of eukaryote feeding modes, cell structural diversity, and classification of the protozoan phyla Loukozoa, Sulcozoa, and Choanozoa. *Eur J Protistol* **49**, 115-178, doi:10.1016/j.ejop.2012.06.001 (2013).

44   Cavalier-Smith, T. in *The Flagellates.*   (eds S. Leadbeater & J. Green) (Taylor and Francis, 2000).

45   Stechmann, A. & Cavalier-Smith, T. Rooting the eukaryote tree by using a derived gene fusion. *Science* **297**, 89-91 (2002).

46   Cavalier-Smith, T. Only six kingdoms of life. *Proceedings of the Royal Society of London Series B-Biological Sciences* **271**, 1251-1262 (2004).

47   Cavalier-Smith, T. Protist phylogeny and the high-level classification of Protozoa. *European Journal of Protistology* **39**, 338-348 (2003).

48   Heiss, A. A., Walker, G. & Simpson, A. G. The flagellar apparatus of Breviata anathema, a eukaryote without a clear supergroup affinity. *Eur J Protistol* **49**, 354-372, doi:10.1016/j.ejop.2013.01.001 (2013).

49   Roger, A. J. & Simpson, A. G. B. Evolution: Revisiting the Root of the Eukaryote Tree. *Current Biology* **19**, R165-R167 (2009).

50   Chistiakova, L. V., Miteva, O. A., Frolov, A. O. & Skarlato, S. O. [Comparative morphology of the subphilum Conosa Cavalier-Smith 1998]. *Tsitologiia* **55**, 778-787 (2013).

51   Derelle, R. *et al.* Bacterial proteins pinpoint a single eukaryotic root. *Proc Natl Acad Sci U S A* **112**, E693-699, doi:10.1073/pnas.1420657112 (2015).

52   Spiegel, F. W. in *Encyclopedia of Evolutionary Biology*   (ed Richard M. Kliman) 325-332 (Academic Press, 2016).

53   Fiz-Palacios, O. *et al.* Did terrestrial diversification of amoebas (amoebozoa) occur in synchrony with land plants? *PLoS One* **8**, e74374, doi:10.1371/journal.pone.0074374 (2013).

54   Schuster, J. J. & Markx, G. H. Biofilm Architecture. . *Advances in Biochemical Engineering/Biotechnology*, 77–96, doi:doi:10.1007/10_2013_248 (2013).

55   Rich, V. I. & Maier, R. M. *Aquatic Environments*. Third Edition edn, (2015).

56   Allwood, A. C., Walter, M. R., Kamber, B. S., Marshall, C. P. & Burch, I. W. Stromatolite reef from the Early Archaean era of Australia. *Nature* **441**, 714-718, doi:10.1038/nature04764 (2006).

57   Noffke, N., Christian, D., Wacey, D. & Hazen, R. M. Microbially induced sedimentary structures recording an ancient ecosystem in the ca. 3.48 billion-year-old Dresser Formation, Pilbara, Western Australia. *Astrobiology* **13**, 1103-1124, doi:10.1089/ast.2013.1030 (2013).

58   Andersson, A. *et al.* Predators and nutrient availability favor protozoa-resisting bacteria in aquatic systems. *Sci Rep* **8**, 8415, doi:10.1038/s41598-018-26422-4 (2018).

59   Matz, C. & Kjelleberg, S. Off the hook--how bacteria survive protozoan grazing. *Trends Microbiol* **13**, 302-307, doi:10.1016/j.tim.2005.05.009 (2005).

60   Andersen, P. & Fenchel, T. Bacterivory by microheterotrophic flagellates in seawater samples. . *Limnol. Oceanogr.* **30**, 198–202. (1985).

61   Fenchel, T. *The Ecology of Heterotrophic Microflagellates.*, Vol. 9 (1986).

62   Purcell, E. M. Life at low Reynolds number. *American Journal of Physics* **45** (1977).

63   Fenchel, T. *Ecology of Protozoa*. (Springer-Verlag, 1987).

64   Butler, H. & Rogerson, A. Consumption rates of six species of marine benthic naked amoebae (Gymnamoebia) from sediments in the Clyde Sea area. . *Journal of the Marine Biological Association of the United Kingdom* **77**, 989-997. (1997).

65   Jackson, S. M. & Jones, E. B. G. Interactions within biofilms: the disruption of biofilm structure by protozoa. *Kieler Meeresforsch. Sonderh.* **8**, 264-268. (1991).

66   Martin, K. H., Borlee, G. I., Wheat, W. H., Jackson, M. & Borlee, B. R. Busting biofilms: free-living amoebae disrupt preformed methicillin-resistant Staphylococcus aureus (MRSA) and Mycobacterium bovis biofilms. . *Microbiology*   **166**, 695. (2020).

67   Jahnke, J., Wehren, T. & Priefer, U. B. vitro studies of the impact of the naked soil amoeba Thecamoeba similis Greef, feeding on phototrophic soil biofilms. . *In Eur J Soil Biol* **43**, 14– 22 (2007).

68   Anderson, O. R. Naked amoebae in biofilms collected from a temperate freshwater pond. *J Eukaryot Microbiol* **60**, 429-431, doi:10.1111/jeu.12042 (2013).

69   Rogerson, A., Anderson, O. R. & Vogel, C. re planktonic naked amoebae predominately floc associated or free in the water column? *Journal of Plankton Research* **25**, 1359–1365 (2003).

70   Parry, J. D. Protozoan grazing of freshwater biofilms. *Adv Appl Microbiol* **54**, 167-196, doi:10.1016/S0065-2164(04)54007-8 (2004).

71   Wang, Y., Coleman-Derr, D., Chen, G. & Gu, Y. Q. OrthoVenn: a web server for genome wide comparison and annotation of orthologous clusters across multiple species. *Nucleic Acids Res* **43**, W78-84, doi:10.1093/nar/gkv487 (2015).

72   Katoh, K. & Standley, D. M. MAFFT multiple sequence alignment software version 7: improvements in performance and usability. *Mol Biol Evol* **30**, 772-780, doi:10.1093/molbev/mst010 (2013).

73   Capella-Gutierrez, S., Silla-Martinez, J. M. & Gabaldon, T. trimAl: a tool for automated alignment trimming in large-scale phylogenetic analyses. *Bioinformatics* **25**, 1972-1973, doi:10.1093/bioinformatics/btp348 (2009).

74   Nguyen, L. T., Schmidt, H. A., von Haeseler, A. & Minh, B. Q. IQ-TREE: a fast and effective stochastic algorithm for estimating maximum-likelihood phylogenies. *Mol Biol Evol* **32**, 268-274, doi:10.1093/molbev/msu300 (2015).

75   Edgar, R. C. Search and clustering orders of magnitude faster than BLAST. *Bioinformatics* **26**, 2460-2461, doi:btq461 [pii] 10.1093/bioinformatics/btq461 (2010).

76   Chen, F., Mackey, A. J., Stoeckert, C. J. J. & Roos, D. S. OrthoMCL-DB: querying a comprehensive multi-species collection of ortholog groups. *Nucleic Acids Res.* **1**, 34, doi:doi: 10.1093/nar/gkj123. (2006).

77   Stamatakis, A., Ludwig, T. & Meier, H. RAxML-III: a fast program for maximum likelihood-based inference of large phylogenetic trees. *Bioinformatics* **21**, 456-463 (2005).

78   Zhou, X. *et al.* Quartet-Based Computations of Internode Certainty Provide Robust Measures of Phylogenetic Incongruence. *Systematic Biology* **69**, 308–324 (2020).

79   Kobert, K., Salichos, L., Rokas, A., Stamatakis, A. & , C. t. I. C. a. R. M. f. P. G. T. Computing the Internode Certainty and Related Measures from Partial Gene Trees. *Molecular Biology and Evolution* **33**, 1606–1617, doi:https://doi.org/10.1093/molbev/msw040 (2016).

80   Shimodaira, H. An approximately unbiased test of phylogenetic tree selection. *Systematic Biology* **51**, 492-508 (2002).

81   Kishino, H., Miyata, T. & Hasegawa, M. Maximum likelihood inference of protein phylogeny and the origin of chloroplasts. ( ). https://doi.org/10.1007/BF02109483. *J Mol Evol* **31**, 151–160 (1990).

Acknowledgments

Author contributions

YIT conceived the project, led writing manuscript and helped design experiments and analysis. FW and FCW collected data, conducted analysis, and contributed to writing and editing of the manuscript. ORA and AS helped with writing, editing and organizing of the manuscript. All authors have read and approved the manuscript.

Competing interests

The authors declare that they have no competing interests.

1 **Figure captions**
2
3 **Figure 1.** Genome wide phylogeny of the Amoebozoa inferred using Maximum
4 likelihood (ML) in IQ-TREE with LG+G4+C60+F model of evolution. The data matrix
5 used to infer this tree consisted of 113,910 amino acid sites from the full dataset, derived
6 from 824 genes and 113 taxa including 10 outgroup taxa. Clade supports at nodes are ML
7 IQ-TREE 1000 ultrafast bootstrap values obtained using the same model. All branches
8 are drawn to scale except a branch leading to Archamoebae, and *Sapocribrum*
9 *chincoteaguense* and *Parvamoeba monoura*, that were reduced to one third and half,
10 respectively.
11
12 **Figure 2.** A scheme illustrating the loss of kinetosomes and cilia under the different
13 evolutionary hypotheses (A and B). Vertical hash marks on branches show loss of
14 kinetosomes (the number lost as designated by labels on the diagram) depending on the
15 lineage.
16
17 **Supplementary Figure caption**
18
19 **Figure S1**. Genome wide phylogeny of the Amoebozoa inferred using Maximum
20 likelihood (ML) in IQ-TREE with LG+G4+C60+F model of evolution. The data matrix
21 used to infer this tree consisted of 93,820 sites amino acid sites with three fast categories
22 of sites (13%) removed from the full dataset. The data matrix consists of 824 genes and
23 113 taxa including 10 outgroup taxa. The topology was estimated
24 under LG+G4+C60+F+PMSF [Y1] model using a guide tree from a topology estimated
25 using full dataset shown in Figure 1. Clade supports at nodes are ML IQ-TREE 1000
26 ultrafast bootstrap values obtained using the same model. All branches are drawn to
27 scale.
28
29 **Figure S2**. Maximum Likelihood tree inferred by RAxML with six fast categories of
30 sites removed from the full dataset. The topology was estimated under
31 PROTGAMMALG4X model. Total number of sites included after removing six fast sites
32 categories is 70,543.
33
34 **Figure S3**. Internode certainty inferred by QuartetScores for topology in Figure 1. Values
35 at branches are Quadripartition internode certainty (qp-ic); Lowest quartet internode
36 certainty (lp-ic); Extended Quadripartition internode certainty (eqp-ic).
37
38 **Figure S4**. Internode certainty inferred using RAxML under PROTGAMMALG4X
39 model for topology in Figure 1. Branch labels showed the internode certainty for a given
40 internode with the most conflicting bipartition (left value) or all conflicting bipartitions
41 (right value). Relative tree certainty including all conflicting bipartitions for this tree is
42 0.978410.